



**HAL**  
open science

## Identification of signaling pathways targeted by the food contaminant FB1: Transcriptome and kinome analysis of samples from pig liver and intestine

Marion Régnier, Pascal Gourbeyre, Philippe Pinton, Scott Napper, Joëlle Laffitte, Anne Marie Cossalter, Jean-Denis Bailly, Yannick Lippi, Justine Bertrand-Michel, Ana-Paula Loureiro-Bracarense, et al.

### ► To cite this version:

Marion Régnier, Pascal Gourbeyre, Philippe Pinton, Scott Napper, Joëlle Laffitte, et al.. Identification of signaling pathways targeted by the food contaminant FB1: Transcriptome and kinome analysis of samples from pig liver and intestine. *Molecular Nutrition and Food Research*, 2017, in press (12), 42 p. 10.1002/mnfr.201700433 . hal-01606651

**HAL Id: hal-01606651**

**<https://hal.science/hal-01606651>**

Submitted on 26 May 2020

**HAL** is a multi-disciplinary open access archive for the deposit and dissemination of scientific research documents, whether they are published or not. The documents may come from teaching and research institutions in France or abroad, or from public or private research centers.

L'archive ouverte pluridisciplinaire **HAL**, est destinée au dépôt et à la diffusion de documents scientifiques de niveau recherche, publiés ou non, émanant des établissements d'enseignement et de recherche français ou étrangers, des laboratoires publics ou privés.

**Title:** Identification of signaling pathways targeted by the food contaminant FB1: transcriptome and kinome analysis of samples from pig liver and intestine

**Authors:** Marion Régnier<sup>\*1</sup>, Pascal Gourbeyre<sup>\*1</sup>, Philippe Pinton<sup>1</sup>, Scott Napper<sup>2,3</sup>, Joëlle Laffite<sup>1</sup>, Anne-Marie Cossalter<sup>1</sup>, Jean-Denis Bailly<sup>1</sup>, Yannick Lippi<sup>1</sup>, Justine Bertrand-Michel<sup>4</sup>, Ana Paula F.R.L. Bracarense<sup>5</sup>, Hervé Guillou<sup>1</sup>, Nicolas Loiseau<sup>#1</sup>, Isabelle P. Oswald<sup>#1</sup>

1 Toxalim (Research Centre in Food Toxicology), Université de Toulouse, INRA, ENVT, INP-Purpan, UPS, Toulouse, France.

2 Vaccine and Infectious Disease Organization - International Vaccine Center, University of Saskatchewan, Saskatoon, Saskatchewan S7N 5E3, Canada.

3 Department of Biochemistry, University of Saskatchewan, Saskatoon, Saskatchewan S7N 5E5, Canada.

4 MetaToul-Lipidomic Facility-MetaboHUB, INSERM UMR1048, Institute of Cardiovascular and Metabolic Diseases, Université Paul Sabatier-Toulouse III, Toulouse, France.

5 Universidade Estadual de Londrina, Laboratory of Animal Pathology, Campus Universitário, Rodovia Celso Garcia Cid, Km 380, Londrina, Paraná 86051-990, Brazil.

\* These authors contributed equally to this work.

Received: 18/05/2017; Revised: 20/07/2017; Accepted: 21/07/2017

This article has been accepted for publication and undergone full peer review but has not been through the copyediting, typesetting, pagination and proofreading process, which may lead to differences between this version and the [Version of Record](#). Please cite this article as [doi: 10.1002/mnfr.201700433](https://doi.org/10.1002/mnfr.201700433).

This article is protected by copyright. All rights reserved.

Comment citer ce document :

Régnier, M., Gourbeyre, P., Pinton, P., Napper, S., Laffite, J., Cossalter, A. M., Bailly, J.-D., Lippi, Y., Bertrand-Michel, J., Bracarense, A. P. F., Guillou, H., Loiseau, N. (Auteur de correspondance), Oswald, I. P. (Auteur de correspondance) (2017). Identification of signaling pathways targeted by the food contaminant FB1: Transcriptome and kinome analysis of samples from

# Correspondence and requests for materials should be addressed either to Nicolas LOISEAU or  
Isabelle OSWALD

Dr. Isabelle P. Oswald, PhD

Toxalim UMR1331 INRA/ENVT/INP/UPS

180, Chemin de Tournefeuille, BP93173, 31027 Toulouse cedex 3 – France

Tel: +33 (0)5 82 06 63 66 ; Fax: +33 (0)5 61 28 52 44

Email: [isabelle.oswald@inra.fr](mailto:isabelle.oswald@inra.fr)

Dr. Nicolas Loiseau, PhD

Toxalim UMR1331 INRA/ENVT/INP/UPS

180, Chemin de Tournefeuille, BP93173, 31027 Toulouse cedex 3 – France

Tel: +33 (0)5 82 06 63 03 ; Fax: +33 (0)5 61 28 52 44

Email: [nicolas.loiseau@inra.fr](mailto:nicolas.loiseau@inra.fr)

Abbreviations: PP2A: protein phosphatase 2; PI3K: phosphoinositide 3-kinase; MYD88 : Myeloid  
differentiation primary response gene 88 ; TLR4: Toll-like receptor 4; NF- $\kappa$ B: Nuclear factor  
kappa B; TNF  $\alpha$ : Tumor necrosis factor-alpha; Protein Kinase B (AKT); Phosphatase and tensin  
homolog (PTEN); Kyoto Encyclopedia of Genes and Genomes (KEGG)

This article is protected by copyright. All rights reserved.

2

Comment citer ce document :

Régnier, M., Gourbeyre, P., Pinton, P., Napper, S., Laffitte, J., Cossalter, A. M., Bailly, J.-D., Lippi, Y., Bertrand-Michel, J., Bracarense, A. P. F., Guillou, H., Loiseau, N. (Auteur de correspondance), Oswald, I. P. (Auteur de correspondance) (2017). Identification of signaling pathways targeted by the food contaminant FB1: Transcriptome and kinome analysis of samples from

## Keywords

Fumonisin, PI3K-AKT signaling, Jejunum, Liver, Swine

## ABSTRACT

**Scope.** Fumonisin B1 (FB1) is a mycotoxin produced by *Fusarium* species. In mammals, this toxin causes widespread organ-specific damage; it promotes hepatotoxicity, is immunotoxic, alters intestinal functions... Despite its inhibitory effect on de novo ceramide synthesis, its molecular mechanism of action and toxicity are not totally elucidated.

**Method & Results.** To explore the mechanism of FB1 toxicity, we analyzed the transcriptome and kinome of two organs targeted by FB1: the liver and the jejunum. Pigs were fed for 4 weeks on a control diet or a FB1-contaminated diet (10 mg/kg). As expected, FB1-exposed pigs gained less weight and displayed a higher sphinganine/sphingosine ratio. Comparison of the transcriptomes and the kinomes of treated versus control pigs showed striking differences. Among the disrupted pathways in liver and jejunum, we highlight Protein Kinase B (AKT) / Phosphatase and tensin homolog (PTEN) at the intersection of the FB1-modulated pathways.

**Conclusion.** Most of the effects of FB1 are mediated by the regulation of ceramide level, which influences protein phosphatase 2 (PP2A) and the phosphoinositide 3-kinase (PI3K)/AKT signaling pathway. This pathway might be a new target to counteract toxic effect of Fumonin B1 which are on of the most spread nutritional's contaminant in the world.

This article is protected by copyright. All rights reserved.

3

Comment citer ce document :

Régnier, M., Gourbeyre, P., Pinton, P., Napper, S., Laffitte, J., Cossalter, A. M., Bailly, J.-D., Lippi, Y., Bertrand-Michel, J., Bracarense, A. P. F., Guillou, H., Loiseau, N. (Auteur de correspondance), Oswald, I. P. (Auteur de correspondance) (2017). Identification of signaling pathways targeted by the food contaminant FB1: Transcriptome and kinome analysis of samples from

**Graphical Abstract:**

FB1 is one of the most spread mycotoxin in the world which induces a broad spectrum of damage in mammals. The molecular mechanism of action of this toxin remaining unclear, so we used a comparative approach with transcriptome and kinome profiles to highlight PP2A and PI3K/AKT as key signaling pathways involved in FB1 toxicity. We assume this key point might be a good target to develop new antimycotoxin strategy in the future.

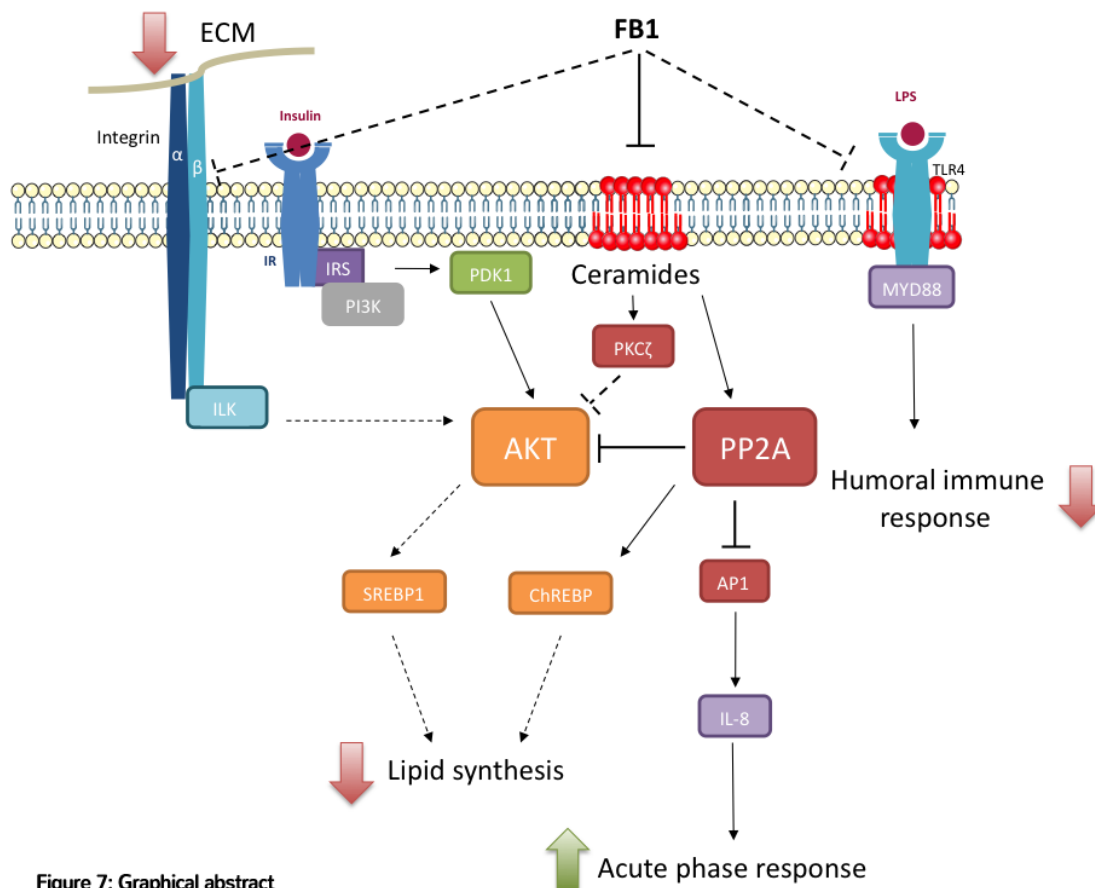


Figure 7: Graphical abstract

## INTRODUCTION

Mycotoxins are toxic secondary metabolite produced by fungi. They are considered to be a major risk factor affecting human and animal health; in addition they lead to considerable economic losses [1]. At more than 800 million tons per year, maize is the cereal with the highest production in the world [2]. This plant, largely used for food and feed, is frequently contaminated by the mycotoxin Fumonisin B1 (FB1). This mycotoxin is mainly produced by *Fusarium verticillioides* and *F. proliferatum*. Global surveys indicate that the worldwide occurrence and levels of FB1 contamination in maize and maize-based products remain very high [3, 4]. The European Scientific Co-operation (SCOOP) task force [3] reported that in the average European country, a third of food analyses show FB1 contamination from 300 to 10 000 µg/Kg. In 2013, in testing 11,600 samples of feed, Schatzmayr and Streit [4] reported that 54% were contaminated with a mean contamination of 1647µg/kg. Although levels up to 77 502 µg /Kg was detected, the great majority (99%) of the samples complied with EU guidance values. In 2006 and 2007, the European Union set recommendations and regulations for the maximum level of FB1 in animal feed and human food [5].

FB1 provokes severe mycotoxicosis in animals through different clinical symptoms [6]; however, in all mammalian species, FB1 elicits nephrotoxicity, hepatotoxicity [6], immunotoxicity [7][8], and intestinal barrier function disturbance [9]. More specific toxicosis have also been reported: leukoencephalomalacia in horses, pulmonary edema and cardiac dysfunction in pigs [10], neural tube defects through effects of FB1 on folate transport in rodents [11], and carcinogenic effects in rodents [6].

As a result of the structural similarity of FB1 with sphingoid base long chains (the backbones of sphingolipids), FB1 disrupts *de novo* sphingolipid metabolism through inhibition of the enzyme ceramide synthase [12]. This inhibition leads to an increase in free sphinganine levels and a decreased content of complex sphingolipids and ceramides. Under these conditions,

This article is protected by copyright. All rights reserved.

5

Comment citer ce document :

Régnier, M., Gourbeyre, P., Pinton, P., Napper, S., Laffitte, J., Cossalter, A. M., Bailly, J.-D., Lippi, Y., Bertrand-Michel, J., Bracarense, A. P. F., Guillou, H., Loiseau, N. (Auteur de correspondance), Oswald, I. P. (Auteur de correspondance) (2017). Identification of signaling pathways targeted by the food contaminant FB1: Transcriptome and kinome analysis of samples from

the ratio of free sphingoid bases (sphinganine/sphingosine; Sa/So) increases in several tissues such as liver or intestine and in plasma and cell lines [9][13][14].

At a molecular level, several targets of FB1 have been identified. For example, FB1 affects the immune system, modulating the expression of proinflammatory cytokines [15] and increasing susceptibility to infection [8][16]. FB1 also restores insulin sensitivity, decreasing the ceramide content by inhibition of their *de novo* synthesis, which is involved in the activation of protein phosphatase 2A (PP2A) repressing the phosphoinositide 3-kinase (PI3K)/Akt signaling pathway [17][18].

For a global view of FB1's molecular effects, in the current work, intestinal and liver samples of pigs exposed to a FB1-contaminated diet were analyzed using untargeted approaches (transcriptomic and kinomic). We provide evidence that most of the effects of FB1 on immunity, carcinogenesis, and lipid metabolism are mediated by the regulation of ceramide level, which influences PP2A and the PI3K/Akt signaling pathway.

## MATERIALS AND METHODS

### Animals

Twelve castrated male pigs (Pietrain/Duroc/Large-white) weaned at 28 days of age were obtained from a local farm (Gaec de Calvignac, St Vincent d'Autejac, France). They were acclimatized for one week in the animal facility of the INRA ToxAlim Unit (Toulouse, France) prior to being used in experimental protocols. Animals were given *ad libitum* access to water and fed. The experiments were carried out in accordance with European Guidelines for the Care and Use of Animals for Research Purposes (accreditation number APAFIS#5917-2016070116429578 v3).

This article is protected by copyright. All rights reserved.

6

Comment citer ce document :

Régnier, M., Gourbeyre, P., Pinton, P., Napper, S., Laffitte, J., Cossalter, A. M., Bailly, J.-D., Lippi, Y., Bertrand-Michel, J., Bracarense, A. P. F., Guillou, H., Loiseau, N. (Auteur de correspondance), Oswald, I. P. (Auteur de correspondance) (2017). Identification of signaling pathways targeted by the food contaminant FB1: Transcriptome and kinome analysis of samples from

### Feeding trial and sampling

Diets were manufactured at INRA facilities in Rennes (France) and formulated according to the energy and amino acid requirements for piglets. Two different batches were prepared, one control batch and one batch artificially contaminated with fumonisin, as previously described [19]. Animals were exposed for 4 weeks to different diets: 6 pigs received the control diet, and 6 pigs the contaminated-diet (10.2 mg FB1 + 2.5 mg FB2 + 1.5 mg FB3/kg). The feed was analyzed for mycotoxin content (Labocea, Ploufragan, France). Deoxynivalenol and zearalenone were naturally present in the cereals used, resulting in concentrations of 0.12 and 0.015 mg/kg feed, respectively. All other mycotoxins, including aflatoxins, T-2 toxin, HT-2 toxin, and ochratoxin A, were below the limits of detection.

Animals were slaughtered by electro-narcosis before exsanguinations. Following euthanasia, samples from jejunum and liver were collected. Samples were fixed in 10% buffered formalin for histopathological analysis or snap-frozen in liquid nitrogen, and stored at -80°C for transcriptome and kinome analysis.

### Determination of tissue lesions and villous morphometry

The tissue pieces were dehydrated through graded alcohols and embedded in paraffin wax. Sections of 3 µm were stained with hematoxylin–eosin (HE, Sigma) for histopathological evaluation. Microscopic observations in jejunum and in ileum were quantified as described [20][21]. A lesion score per animal was established by taking into account the importance degree of the lesion (severity factor) and its extent (intensity or observed frequency). Morphometry was evaluated in the jejunum by measuring the villi height randomly on 30 villi using a MOTIC Image Plus 2.0 ML® image analysis system, as described [20][21]. The slides

were observed in a blind way by the same pathologist and irrespective of the experimental groups.

### Gene expression analysis

For the gene expression analysis, total RNA was extracted in lysing matrix D tubes (MP Biomedicals, Illkirch, France) containing guanidine thiocyanate-acid phenol (Eurobio). RNA quality was confirmed using a kit (Agilent RNA 6000 Nano Kit Quick, Agilent Bioanalyzer 2100). Reverse transcription and RT-qPCR steps were performed as already described [22] with previously published primers (Supplementary Table S1) [23][24]. Amplification efficiency and initial fluorescence were determined by the  $\Delta$ Ct method. Obtained values were normalized using two reference genes, ribosomal protein L32 and cyclophilin A. Gene expression levels of treated samples were expressed relative to the mean of the control ones.

### Anti-*Mycoplasma hyopneumoniae* vaccination

On the first and eighth days of the experiment, all piglets were immunized by subcutaneous inoculation with 2 ml of anti *M. hyopneumoniae* vaccine (Stellamune®, Pfizer Animal Health, Rueil-Malmaison, France) as already described [25]. At weekly time intervals, blood samples were aseptically collected. The presence of specific IgG antibodies against *M. hyopneumoniae* was quantified using a commercial ELISA kit (ID Screen® *Mycoplasma hyopneumoniae* Indirect, Montpellier, France).

### **Sphingoid base determination level ratio**

The ratio of the sphingoid base Sphinganine over Sphingosine (Sa/So) has been determined in the liver after a regular Bligh and Dyer extraction and analysis as previously described by Loiseau *et al.*, in 2007 [9].

### **Biochemical assays**

Plasma levels of triglycerides, total cholesterol, and low- or high-density lipoprotein (LDL, HDL) cholesterol were determined on a biochemical analyzer, COBAS-MIRA+.

### **Gene expression analysis by microarray**

The microarray GPL16524 (Agilent Technology, 8 × 60K) used in this experiment consisted of 43,603 spots derived from the 44K (V2:026440 design) Agilent porcine-specific microarray and completed with 9532 genes from adipose tissue, 3776 genes from the immune system, and 3768 genes from skeletal muscle [26]. For each sample, Cyanine-3 (Cy3)-labeled cRNA was prepared as already described [29]. Slides were scanned immediately after washing on an Agilent G2505C Microarray Scanner with Agilent Scan Control A.8.5.1 software. All experimental details are available in the Gene Expression Omnibus (GEO) database under accession GSE97818 and GSE97817 (<https://www.ncbi.nlm.nih.gov/geo/query/acc.cgi?token=gbilagkijzudpyt&acc=GSE97818> and <https://www.ncbi.nlm.nih.gov/geo/query/acc.cgi?token=udajaoginlqxjyd&acc=GSE97817>). The differentially expressed genes (adjusted  $P \leq 0.05$ ) were hierarchically clustered and visualized in heatmaps.

This article is protected by copyright. All rights reserved.

9

Comment citer ce document :

Régnier, M., Gourbeyre, P., Pinton, P., Napper, S., Laffitte, J., Cossalter, A. M., Bailly, J.-D., Lippi, Y., Bertrand-Michel, J., Bracarense, A. P. F., Guillou, H., Loiseau, N. (Auteur de correspondance), Oswald, I. P. (Auteur de correspondance) (2017). Identification of signaling pathways targeted by the food contaminant FB1: Transcriptome and kinome analysis of samples from

### **Peptide arrays and kinome analysis**

Design, construction, and application of the peptide arrays were performed using a modified version of a previously described protocol [27]. Protocol details are provided in supplementary material file. Focusing on differences between samples, fold-change values were calculated for each peptide, as described previously [28], to determine whether phosphorylation was significantly different in a given pair of treated and untreated tissues. To analyze differences at a broader level, the pathway database and analysis tool InnateDB [29] was used as described previously [30] to identify pathways that were upregulated or downregulated.

### **Construction of the protein–protein interaction network**

To further investigate the molecular mechanism of FB1, a protein–protein interaction (PPI) network of the differentially expressed genes and the differentially phosphorylated proteins was constructed (<http://www.string-db.org/>). Here, we selected gene–gene interactions with integrated scores greater than 0.4 (the default threshold in the STRING database) or highest confidence (0.9) to construct the PPI network and visualize it [31]. After PPI building, results were analyzed and Kyoto Encyclopedia of Genes and Genomes (KEGG) functional enrichment results of the highlighted network reported.

### **Statistical analysis**

Principal component analysis was used to determine if patterns of samples from FB1- exposed animals were distinct from those of control animal samples. To identify common phosphorylated peptides from different organs, Venn analysis was performed. Data were

This article is protected by copyright. All rights reserved.

10

processed using R ([www.r-project.org](http://www.r-project.org)) for principal component and Venn analyses. For visual interpretation, peptides were input with their fold-change values into Innate DB [29]. This software was used as described previously [30] to identify pathways that were upregulated or downregulated. Functional analysis of differentially expressed genes was performed using the Ingenuity Pathway Analysis (IPA) tool (<http://www.ingenuity.com>) to identify pathways and processes affected by toxins.

## RESULTS AND DISCUSSION

### Effects of FB1 on physiological parameters

The effect of FB1 on physiological parameters was first assessed. Throughout the experiment, a significant difference in weight gain was observed between animals receiving the control and the FB1-contaminated diets (Fig. 1A). Such an effect has already been reported in animals exposed to 8 mg FB1/kg feed [32]. The decreased weight gain has been associated with a decreased feed consumption, a phenomenon that is common in pigs exposed to contaminated feed because of their efficient olfactory organ.

At the end of the experiment, liver and jejunum were sampled for biochemical and histological analysis. As expected, an increase in the Sa/So ratio was observed in animals receiving the FB1-contaminated diet (Fig. 1B). The Sa/So ratio is a pertinent marker of exposure to FB1 in the liver, which reveals an accumulation of sphinganine due to inhibition of ceramide synthase proteins involved in ceramide *de novo* synthesis. Several groups have already reported an increase in this ratio in animals exposed to FB1 [33][34][35].

Finally, the measurement of the size of villus height in two segments of the intestine (jejunum and ileum) showed a decrease in villi length among animals fed FB1 (Fig. 1C). As  
This article is protected by copyright. All rights reserved.

Bracarense et al. suggested in 2012 [36], the decrease in villi height could reflect an inhibitory effect of FB1 on cell differentiation. Overall, these data are in agreement with previously reported literature on the effects of FB1 exposure.

### **Analysis of FB1 effects by a transcriptomic untargeted approach**

As a first untargeted approach, a genome-wide transcriptomic analysis was performed to investigate the global effect of FB1 (Fig. 2). Exposure to the toxin resulted in differential expression of 196 genes, corresponding to 49 and 74 genes up- and downregulated, respectively, in the jejunum and to 31 and 42 genes up- and downregulated, respectively, in the liver.

As shown in Table 1, in the jejunum of FB1-treated animals, the most significantly regulated genes (fold change greater than 2.5) were related to cell structure (FLNA, ACTA1, DES, SPIRE2); cellular energy (CKM, ANGPT4, FABP6, FABP3); immunity (SLA-DQB1, OASL); metallothioneins (MT1A, MT1G); calcium homeostasis (S100G); and cyclin modulation (CCND1). In the liver (Table 2), the most significantly regulated genes were also related to cell structure genes (COL1A2, COL3A1); cellular energy (ACSL4, IGFBP2, IGF1, SDS, MFSD2A); defense response (PR39, NPG4, ARG1); cation homeostasis (S100A8, S100G, KCNK5); and metallothioneins (MT1A).

Differential expression of genes upon exposure to FB1 was evaluated using IPA software (Tables 3 and 4). FB1 disturbs several pathways, especially: i) ILK signaling in jejunum through the modulation of genes such as fibronectin (FN1), myosin (MYH11), cyclin D1(CCND1), filamin (FLNA, FLNC), and actin (ACTA1, ACTC1, ACTA2); ii) the LXR/RXR activation pathway both in jejunum and liver through the modulation of genes such as ABCG8, SCD, and FASN; and iii)

acute-phase response signaling in jejunum and liver through the modulation of genes such as Myeloid differentiation primary response gene 88 (MYD88), IL-1A, and IL-1R1.

### **Analysis of FB1 effects by an untargeted kinomic approach**

To confirm and refine the data obtained by the transcriptomic untargeted method, an untargeted kinomic approach was performed in parallel. As indicated in Table 5, the jejunum of pigs exposed to FB1 displayed an increased phosphorylation of peptides corresponding to 45 proteins (56 phosphorylation sites) and a decrease in phosphorylation of peptides corresponding to 45 proteins (55 phosphorylation sites). The livers of these animals presented increased phosphorylation of peptides corresponding to 26 proteins (28 phosphorylation sites) and decreased phosphorylation of peptides corresponding to 33 proteins (34 phosphorylation sites).

Some proteins related to the ILK signaling pathway had either increased phosphorylation (Akt1(T308), PTEN(T382/3/5)) in the liver or decreased phosphorylation in this organ (Akt1(S473), PDK1(S241), PI3K p85 $\beta$ (Y605), PIK3R1(Y556), NF- $\kappa$ B p100(S99)) and in the jejunum (Akt1(T308), PTEN(Y240), PI3K p85 $\beta$ (Y605), PIK3R1(Y556), NF- $\kappa$ B-p65(S276), NF- $\kappa$ B-p105(S337)). Similarly, many proteins associated with the cell cycle demonstrated increased phosphorylation in the organs from pigs exposed to FB1, which was notably the case for Cdc2, CDK2, EP300, and Grb10, all involved in cell proliferation.

### **Network analysis**

Protein network analysis was used to establish direct or indirect PPI in the pathways regulated by FB1 in the jejunum and the liver. As shown in Figure 2, two different networks (one for each tissue) have been characterized based on the differentially expressed genes in response to FB1. This article is protected by copyright. All rights reserved.

exposure. Five common enriched KEGG pathways, inside the top 15, were identified both in the jejunum and the liver: i) metabolic pathways; ii) biosynthesis of amino acids; iii) focal adhesion; iv) ECM-receptor interaction; and v) the PI3K-Akt signaling pathway. Tight junction and fatty acid metabolism pathways were also highlighted in jejunum and liver, respectively. As shown in Figures 3 and 4, kinome modulations induced by FB1 exposure were centered on AKT1 and PTEN (in jejunum and liver). In the jejunum, we focused on four significantly regulated pathways from the top 10 (highlighted by the KEGG enrichment analysis) that were mostly regulated by FB1 exposure: i) the Toll-like receptor (TLR) signaling pathway (concerning 16 proteins with a false discovery rate =  $1.19e-21$ ) (Fig. 3E); ii) the PI3K-AKT signaling pathway (19 proteins;  $6.76e-20$ ) (Fig. 3C); iii) the NF- $\kappa$ B signaling pathway (10 proteins;  $2.04e-12$ ) (Fig. 3D); and iv) regulation of actin cytoskeleton (10 proteins;  $7.6e-09$ ) (Fig. 3B). In the liver, KEGG enrichment analysis identified three of the four same pathways significantly modulated by FB1 exposure (Fig. 4), with actin signaling pathways as the exception.

Cross-comparing the protein network analysis reported above, three major common pathways have been characterized as being significantly modulated by FB1 exposure: i) integrin signaling; ii) fatty acid metabolism; and iii) acute-phase response.

## Integrin

As indicated above, FB1 activates ILK signaling. The focal adhesion and the ECM-receptor interactions have been identified as part of the regulated biological system in the presence of FB1. Moreover, the kinome data showed regulation of the actin-signaling pathway in the jejunum. The results from the untargeted approach are in accordance with the observation of a decrease in villi length in animals exposed to FB1 (Fig. 1), which reflects an inhibitory effect of FB1 on cell differentiation. The findings are also in accordance with several publications reporting that FB1 inhibits integrin-mediated cell-matrix adhesion. Indeed, FB1, in inhibiting

This article is protected by copyright. All rights reserved.

ceramide synthesis, depletes rafts in ceramide and disrupts PI3K/AKT signaling. These events result in a decrease in proliferation and in cell–cell or cell–matrix adhesion [37][38][39].

### **Fatty acid metabolism**

The second pathway revealed by the transcriptome and kinome analyses involves fatty acid metabolism. PI3K-AKT signaling, a well-known downstream pathway of the insulin response, is involved in fatty acid metabolism homeostasis through activation of the SREBP1C transcription factor, which modulates genes such as ABCG8, SCD, and FASN. SREBP1C, LXR, and ChREBP are three transcription factors that co-regulate each other to control hepatic lipogenesis [40]. Indeed, LXR can downregulate the PI3K-AKT signaling pathway through inhibition of the phosphorylation of p85 or activation of PTEN.

To confirm these results at a biochemical level, plasma concentrations of cholesterol, LDL, and HDL were measured. As seen in Figure 5, cholesterol, LDL, and HDL – three markers related to LXR-stimulated lipogenesis – increased significantly after 14 and 21 days of exposure to FB1; only triglycerides showed a significant increase after 28 days of exposure. These results support the concept of dysregulation of fatty acid metabolism by FB1. This modulation of lipid homeostasis might be linked to the effect of FB1 on the ceramide pathway. Indeed, an accumulation of ceramides activates PP2A, resulting in inhibition of Akt [41]. In the jejunum, downregulation of lipid and lipoprotein metabolism would be expected; indeed, by inhibiting ceramide synthase, FB1 would block the biosynthesis of complex sphingolipids, disturbing lipid metabolism [42].

## FB1 and the acute-phase response

The third major pathway regulated by FB1 is the acute-phase response. This pathway was identified in IPA analysis of the jejunum transcriptomic experiment. KEGG enrichment also highlighted the involvement of tight junction protein interactions in the jejunum response to FB1 exposure. Likewise, analysis of the kinome by string-db revealed in both jejunum and liver the involvement of the Nuclear factor kappa B (NF- $\kappa$ B) and Toll-like receptor signaling pathways [43]. All of these pathways are closely connected to regulation of immunity.

To confirm the involvement of FB1 in the acute-phase response, the relative mRNA expression levels of several immune markers (Toll-like receptor 4 (TLR4), MYD88, Nuclear factor kappa B (NF- $\kappa$ B), IL-1 $\alpha$ , IL-1 $\beta$ , IL-8, and TNF  $\alpha$ ) were analyzed. As shown in Figure 6A, the expression of TLR4 and MYD88 significantly decreased in the jejunum of FB1-treated animals whereas the expression of NF- $\kappa$ B and IL-8 significantly increased. IL-8 was the only proinflammatory cytokine that increased, an increase that can be explained by the inhibition of *de novo* synthesis of ceramides by FB1. Indeed, ceramide activates PP2A, a serine/threonine phosphatase involved in the negative regulation of TNF  $\alpha$ -induced IL-8 production [44]. Thus, inhibition of ceramide by FB1 induces overexpression of the IL-8 chemokine and consequently NF- $\kappa$ B.

The decreased expression of TLR4 and MYD88 is in accordance with previous results from our group showing that FB1 disturbs the development of the humoral immune response and antibody production [45][46]. In the present experiment, we confirmed the effect of FB1 on the antibody response (Fig. 6B). In contrast to control animals, FB1-exposed pigs produced 10 times less antibody than control animals upon two injections (at D0 and D8) of an anti *M. hyopneumoniae* vaccine. The decreased expression of TLR4 and MYD88 could be explained by the FB1-related decrease in ceramide. Ceramide is involved in the raft membrane complex that is necessary for the appropriate signaling of the TLR4 pathway [47][48].

This article is protected by copyright. All rights reserved.

16

Comment citer ce document :

Régnier, M., Gourbeyre, P., Pinton, P., Napper, S., Laffitte, J., Cossalter, A. M., Bailly, J.-D., Lippi, Y., Bertrand-Michel, J., Bracarense, A. P. F., Guillou, H., Loiseau, N. (Auteur de correspondance), Oswald, I. P. (Auteur de correspondance) (2017). Identification of signaling pathways targeted by the food contaminant FB1: Transcriptome and kinome analysis of samples from

## CONCLUSION

These results indicate that most of the pathways affected by FB1 are related to PI3K-AKT signaling. This finding is of particular interest because FB1 is known to alter sphingolipid/ceramide signaling pathways that modulate PI3K-AKT signaling cascades [49][50]. Indeed, an accumulation of ceramides activates PP2A and PKC $\zeta$ , resulting in an inhibition of AKT; thus, FB1 which induces a decrease in a ceramides level allow AKT to stay available to restores or influences the insulin signals and lipogenesis. Moreover, this PI3K-AKT disturbance induces inhibition of the integrin-mediated cell-matrix adhesion. Finally, this perturbation of the PI3K-AKT signaling pathway could be responsible at least in part for the inflammatory response.

## ACKNOWLEDGMENTS

This study was supported by the ANR Fumolip (ANR-16-CE21-0003) and ANR LipoReg (ANR-15-Carn0016) France.

MR was supported by a Fellowship from the Ministère de l'Éducation Nationale, de la Recherche et de la Technologie.

## Conflict of interest

The authors declare that they have no conflict of interest.

This article is protected by copyright. All rights reserved.

17

Comment citer ce document :

Régnier, M., Gourbeyre, P., Pinton, P., Napper, S., Laffitte, J., Cossalter, A. M., Bailly, J.-D., Lippi, Y., Bertrand-Michel, J., Bracarense, A. P. F., Guillou, H., Loiseau, N. (Auteur de correspondance), Oswald, I. P. (Auteur de correspondance) (2017). Identification of signaling pathways targeted by the food contaminant FB1: Transcriptome and kinome analysis of samples from

**REFERENCES**

- [1] Cano, P.M., Puel, O., Oswald, I.P., Mycotoxins: Fungal Secondary Metabolites with Toxic Properties, in: *Fungi: Applications and Management Strategies*, CRC Press, 2016, pp. 318–371.
- [2] Grain: World Markets and Trade. 2017.
- [3] SCOOP (Scientific Cooperation on Questions to Food) Task 3.2.10 Collection of occurrence data of Fusarium toxins in food and assessment of dietary intake by the population of EU member states. Subtask III: Fumonisin. 2003.
- [4] Streit, E., Naehrer, K., Rodrigues, I., Schatzmayr, G., Mycotoxin occurrence in feed and feed raw materials worldwide: long-term analysis with special focus on Europe and Asia. *J. Sci. Food Agric.* 2013, *93*, 2892–2899.
- [5] Commission Regulation (EC) No 1126/2007 of 28 September 2007 setting maximum levels for certain contaminants in foodstuffs as regards Fusarium toxins in maize and maize products. *Off. J. Eur. Union* 2007, *1126/2007*.
- [6] Bolger, M., Coker, R., DiNovi, M., Gaylor, D., et al., Fumonisin. In: Safety Evaluation of Certain Mycotoxins in Food, in: *WHO Food Additives Series 47*, Geneva 2001.
- [7] Devriendt, B., Gallois, M., 'lanie, Verdonck, F., Wache, Y., et al., The food contaminant fumonisin B(1) reduces the maturation of porcine CD11R1(+) intestinal antigen presenting cells and antigen-specific immune responses, leading to a prolonged intestinal ETEC infection. *Vet. Res.* 2009, *40*, 40.
- [8] Halloy, D.J., Gustin, P.G., Bouhet, S., Oswald, I.P., Oral exposure to culture material extract containing fumonisins predisposes swine to the development of pneumonitis caused by
- This article is protected by copyright. All rights reserved.

Pasteurellamultocida. *Toxicology* 2005, 213, 34–44.

[9] Loiseau, N., Debrauwer, L., Sambou, T., Bouhet, S., et al., Fumonisin B1 exposure and its selective effect on porcine jejunal segment: sphingolipids, glycolipids and trans-epithelial passage disturbance. *Biochem. Pharmacol.* 2007, 74, 144–152.

[10] Haschek, W.M., Gumprecht, L.A., Smith, G., Tumbleson, M.E., et al., Fumonisin toxicosis in swine: an overview of porcine pulmonary edema and current perspectives. *Environ. Health Perspect.* 2001, 109 Suppl 2, 251–257.

[11] Marasas, W.F.O., Riley, R.T., Hendricks, K.A., Stevens, V.L., et al., Fumonisin disrupt sphingolipid metabolism, folate transport, and neural tube development in embryo culture and in vivo: a potential risk factor for human neural tube defects among populations consuming fumonisin-contaminated maize. *J. Nutr.* 2004, 134, 711–716.

[12] Wang, E., Norred, W.P., Bacon, C.W., Riley, R.T., et al., Inhibition of sphingolipid biosynthesis by fumonisins. Implications for diseases associated with *Fusarium moniliforme*. *J. Biol. Chem.* 1991, 266, 14486–14490.

[13] Grenier, B., Bracarense, A.-P.F.L., Schwartz, H.E., Trumel, C., et al., The low intestinal and hepatic toxicity of hydrolyzed fumonisin B<sub>1</sub> correlates with its inability to alter the metabolism of sphingolipids. *Biochem. Pharmacol.* 2012, 83, 1465–1473.

[14] Riley, R.T., An, N.H., Showker, J.L., Yoo, H.S., et al., Alteration of tissue and serum sphinganine to sphingosine ratio: an early biomarker of exposure to fumonisin-containing feeds in pigs. *Toxicol. Appl. Pharmacol.* 1993, 118, 105–112.

[15] Osuchowski, M.F., Edwards, G.L., Sharma, R.P., Fumonisin B1-induced neurodegeneration in mice after intracerebroventricular infusion is concurrent with disruption of sphingolipid metabolism and activation of proinflammatory signaling. *Neurotoxicology* 2005, 26, 211–221.

[16] Oswald, I.P., Desautels, C., Laffitte, J., Fournout, S., et al., Mycotoxin fumonisin B1  
This article is protected by copyright. All rights reserved. 19

Comment citer ce document :

Régnier, M., Gourbeyre, P., Pinton, P., Napper, S., Laffitte, J., Cossalter, A. M., Bailly, J.-D., Lippi, Y., Bertrand-Michel, J., Bracarense, A. P. F., Guillou, H., Loiseau, N. (Auteur de correspondance), Oswald, I. P. (Auteur de correspondance) (2017). Identification of signaling pathways targeted by the food contaminant FB1: Transcriptome and kinome analysis of samples from

increases intestinal colonization by pathogenic *Escherichia coli* in pigs. *Appl. Environ. Microbiol.* 2003, *69*, 5870–5874.

[17] Summers, S.A., Ceramides in insulin resistance and lipotoxicity. *Prog. Lipid Res.* 2006, *45*, 42–72.

[18] Bikman, B.T., Summers, S.A., Ceramides as modulators of cellular and whole-body metabolism. *J. Clin. Invest.* 2011, *121*, 4222–4230.

[19] Meissonnier, G.M., Laffitte, J., Raymond, I., Benoit, E., et al., Subclinical doses of T-2 toxin impair acquired immune response and liver cytochrome P450 in pigs. *Toxicology* 2008, *247*, 46–54.

[20] Luciola, J., Pinton, P., Callu, P., Laffitte, J., et al., The food contaminant deoxynivalenol activates the mitogen activated protein kinases in the intestine: interest of ex vivo models as an alternative to in vivo experiments. *Toxicon* 2013, *66*, 31–36.

[21] Gerez, J.R., Pinton, P., Callu, P., Grosjean, F., et al., Deoxynivalenol alone or in combination with nivalenol and zearalenone induce systemic histological changes in pigs. *Exp. Toxicol. Pathol. Off. J. Ges. Toxikol. Pathol.* 2015, *67*, 89–98.

[22] Gourbeyre, P., Berri, M., Lippi, Y., Meurens, F., et al., Pattern recognition receptors in the gut: analysis of their expression along the intestinal tract and the crypt/villus axis. *Physiol. Rep.* 2015, *3*.

[23] Pierron, A., Mimoun, S., Murate, L.S., Loiseau, N., et al., Intestinal toxicity of the masked mycotoxin deoxynivalenol-3- $\beta$ -D-glucoside. *Arch. Toxicol.* 2016, *90*, 2037–2046.

[24] Alassane-Kpembi, I., Puel, O., Pinton, P., Cossalter, A.-M., et al., Co-exposure to low doses of the food contaminants deoxynivalenol and nivalenol has a synergistic inflammatory effect on intestinal explants. *Arch. Toxicol.* 2017, in press.

[25] Mach, N., Gao, Y., Lemonnier, G., Lecardonnell, J., et al., The peripheral blood transcriptome

reflects variations in immunity traits in swine: towards the identification of biomarkers. *BMC Genomics* 2013, *14*, 894.

[26] Pierron, A., Mimoun, S., Murate, L.S., Loiseau, N., et al., Microbial biotransformation of DON: molecular basis for reduced toxicity. *Sci. Rep.* 2016, *6*, 29105.

[27] Jalal, S., Arsenault, R., Potter, A.A., Babiuk, L.A., et al., Genome to kinome: species-specific peptide arrays for kinome analysis. *Sci. Signal.* 2009, *2*, p11.

[28] Trost, B., Kindrachuk, J., Määttänen, P., Napper, S., et al., PIIKA 2: an expanded, web-based platform for analysis of kinome microarray data. *PLoS One* 2013, *8*, e80837.

[29] Lynn, D.J., Winsor, G.L., Chan, C., Richard, N., et al., InnateDB: facilitating systems-level analyses of the mammalian innate immune response. *Mol. Syst. Biol.* 2008, *4*, 218.

[30] Arsenault, R.J., Li, Y., Maattanen, P., Scruten, E., et al., Altered Toll-like receptor 9 signaling in *Mycobacterium avium* subsp. *paratuberculosis*-infected bovine monocytes reveals potential therapeutic targets. *Infect. Immun.* 2013, *81*, 226–237.

[31] Szklarczyk, R., Megchelenbrink, W., Cizek, P., Ledent, M., et al., WeGET: predicting new genes for molecular systems by weighted co-expression. *Nucleic Acids Res.* 2016, *44*, D567-573.

[32] Haschek, W.M., Motelin, G., Ness, D.K., Harlin, K.S., et al., Characterization of fumonisin toxicity in orally and intravenously dosed swine. *Mycopathologia* 1992, *117*, 83–96.

[33] Loiseau, N., Polizzi, A., Dupuy, A., Therville, N., et al., New insights into the organ-specific adverse effects of fumonisin B1: comparison between lung and liver. *Arch. Toxicol.* 2015, *89*, 1619–1629.

[34] Szabó, A., Szabó-Fodor, J., Fébel, H., Mézes, M., et al., Oral administration of fumonisin B1 and T-2 individually and in combination affects hepatic total and mitochondrial membrane lipid profile of rabbits. *Physiol. Int.* 2016, *103*, 321–333.

This article is protected by copyright. All rights reserved.

21

Comment citer ce document :

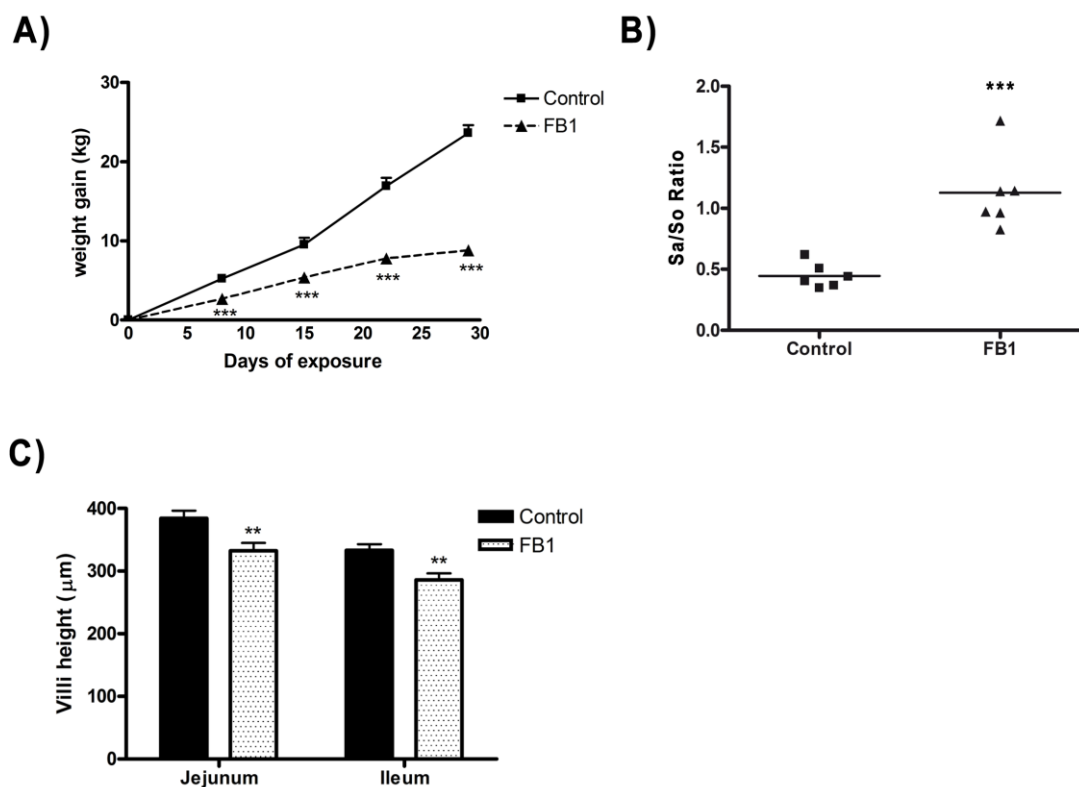
Régnier, M., Gourbeyre, P., Pinton, P., Napper, S., Laffitte, J., Cossalter, A. M., Bailly, J.-D., Lippi, Y., Bertrand-Michel, J., Bracarense, A. P. F., Guillou, H., Loiseau, N. (Auteur de correspondance), Oswald, I. P. (Auteur de correspondance) (2017). Identification of signaling pathways targeted by the food contaminant FB1: Transcriptome and kinome analysis of samples from

- [35] Riedel, S., Abel, S., Burger, H.-M., van der Westhuizen, L., et al., Differential modulation of the lipid metabolism as a model for cellular resistance to fumonisin B1-induced cytotoxic effects in vitro. *Prostaglandins Leukot. Essent. Fatty Acids* 2016, *109*, 39–51.
- [36] Bracarense, A.-P.F.L., Lucioli, J., Grenier, B., Drociunas Pacheco, G., et al., Chronic ingestion of deoxynivalenol and fumonisin, alone or in interaction, induces morphological and immunological changes in the intestine of piglets. *Br. J. Nutr.* 2012, *107*, 1776–1786.
- [37] Decker, L., French-Constant, C., Lipid rafts and integrin activation regulate oligodendrocyte survival. *J. Neurosci.* 2004, *24*, 3816–3825.
- [38] Lee, Y.G., Lee, J., Cho, J.Y., Cell-permeable ceramides act as novel regulators of U937 cell-cell adhesion mediated by CD29, CD98, and CD147. *Immunobiology* 2010, *215*, 294–303.
- [39] Pelagalli, A., Belisario, M.A., Squillacioti, C., Della Morte, R., et al., The mycotoxin fumonisin B1 inhibits integrin-mediated cell-matrix adhesion. *Biochimie* 1999, *81*, 1003–1008.
- [40] Wang, Y., Viscarra, J., Kim, S.-J., Sul, H.S., Transcriptional regulation of hepatic lipogenesis. *Nat. Rev. Mol. Cell Biol.* 2015, *16*, 678–689.
- [41] Mahfouz, R., Khoury, R., Blachnio-Zabielska, A., Turban, S., et al., Characterising the inhibitory actions of ceramide upon insulin signaling in different skeletal muscle cell models: a mechanistic insight. *PLoS One* 2014, *9*, e101865.
- [42] Merrill, A.H., Sullards, M.C., Wang, E., Voss, K.A., et al., Sphingolipid metabolism: roles in signal transduction and disruption by fumonisins. *Environ. Health Perspect.* 2001, *109 Suppl 2*, 283–289.
- [43] Arce, C., Ramírez-Boo, M., Lucena, C., Garrido, J.J., Innate immune activation of swine intestinal epithelial cell lines (IPEC-J2 and IPI-2I) in response to LPS from *Salmonella typhimurium*. *Comp. Immunol. Microbiol. Infect. Dis.* 2010, *33*, 161–174.

- [44] Cornell, T.T., Hinkovska-Galcheva, V., Sun, L., Cai, Q., et al., Ceramide-dependent PP2A regulation of TNF $\alpha$ -induced IL-8 production in respiratory epithelial cells. *Am. J. Physiol. Lung Cell. Mol. Physiol.* 2009, 296, L849-856.
- [45] Taranu, I., Marin, D.E., Bouhet, S., Pascale, F., et al., Mycotoxin fumonisin B1 alters the cytokine profile and decreases the vaccinal antibody titer in pigs. *Toxicol. Sci. Off. J. Soc. Toxicol.* 2005, 84, 301–307.
- [46] Marin, D.E., Taranu, I., Pascale, F., Lionide, A., et al., Sex-related differences in the immune response of weanling piglets exposed to low doses of fumonisin extract. *Br. J. Nutr.* 2006, 95, 1185–1192.
- [47] Lu, D.-Y., Chen, H.-C., Yang, M.-S., Hsu, Y.-M., et al., Ceramide and Toll-like receptor 4 are mobilized into membrane rafts in response to *Helicobacter pylori* infection in gastric epithelial cells. *Infect. Immun.* 2012, 80, 1823–1833.
- [48] Kwon, O.S., Tanner, R.E., Barrows, K.M., Runtsch, M., et al., MyD88 regulates physical inactivity-induced skeletal muscle inflammation, ceramide biosynthesis signaling, and glucose intolerance. *Am. J. Physiol. Endocrinol. Metab.* 2015, 309, E11-21.
- [49] Ramljak, D., Calvert, R.J., Wiesenfeld, P.W., Diwan, B.A., et al., A potential mechanism for fumonisin B(1)-mediated hepatocarcinogenesis: cyclin D1 stabilization associated with activation of Akt and inhibition of GSK-3 $\beta$  activity. *Carcinogenesis* 2000, 21, 1537–1546.
- [50] Hannun, Y.A., Obeid, L.M., Principles of bioactive lipid signalling: lessons from sphingolipids. *Nat. Rev. Mol. Cell Biol.* 2008, 9, 139–150.

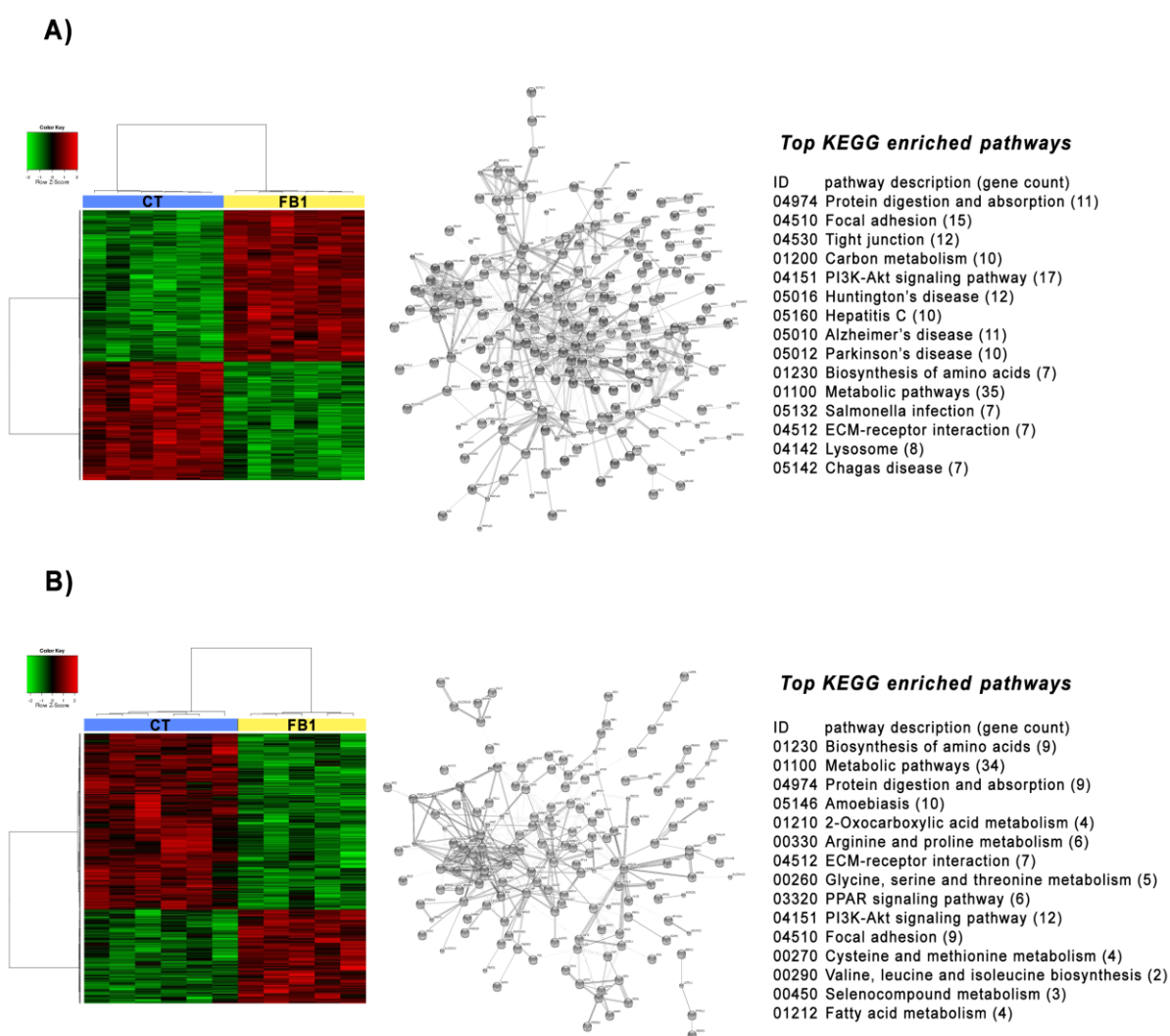
## FIGURE LEGENDS

Figure 1. Animal parameters follow-up with FB1 exposure. (A) Animal body weight-gain. Squares and the solid curve represent the control group whereas triangles and the dashed curve represent the group exposed to FB1 over 28 days (mean means  $\pm$  SD of six animals). (B) Animal liver Sa/So ratio, one of the most predictive biomarkers of FB1 exposure. Each square represents the value of one animal control, and each triangle represents the value of one FB1-exposed. (C) Villi height in two intestinal segments (jejunum and ileum). Data (means  $\pm$  SD of six animals) are plotted with a black solid bar for the control group and a white open dotted bar for the FB1-exposed group. \*\*, and \*\*\* indicate significant differences relative to the control group at  $P < 0.01$ , and  $< 0.001$ , respectively.



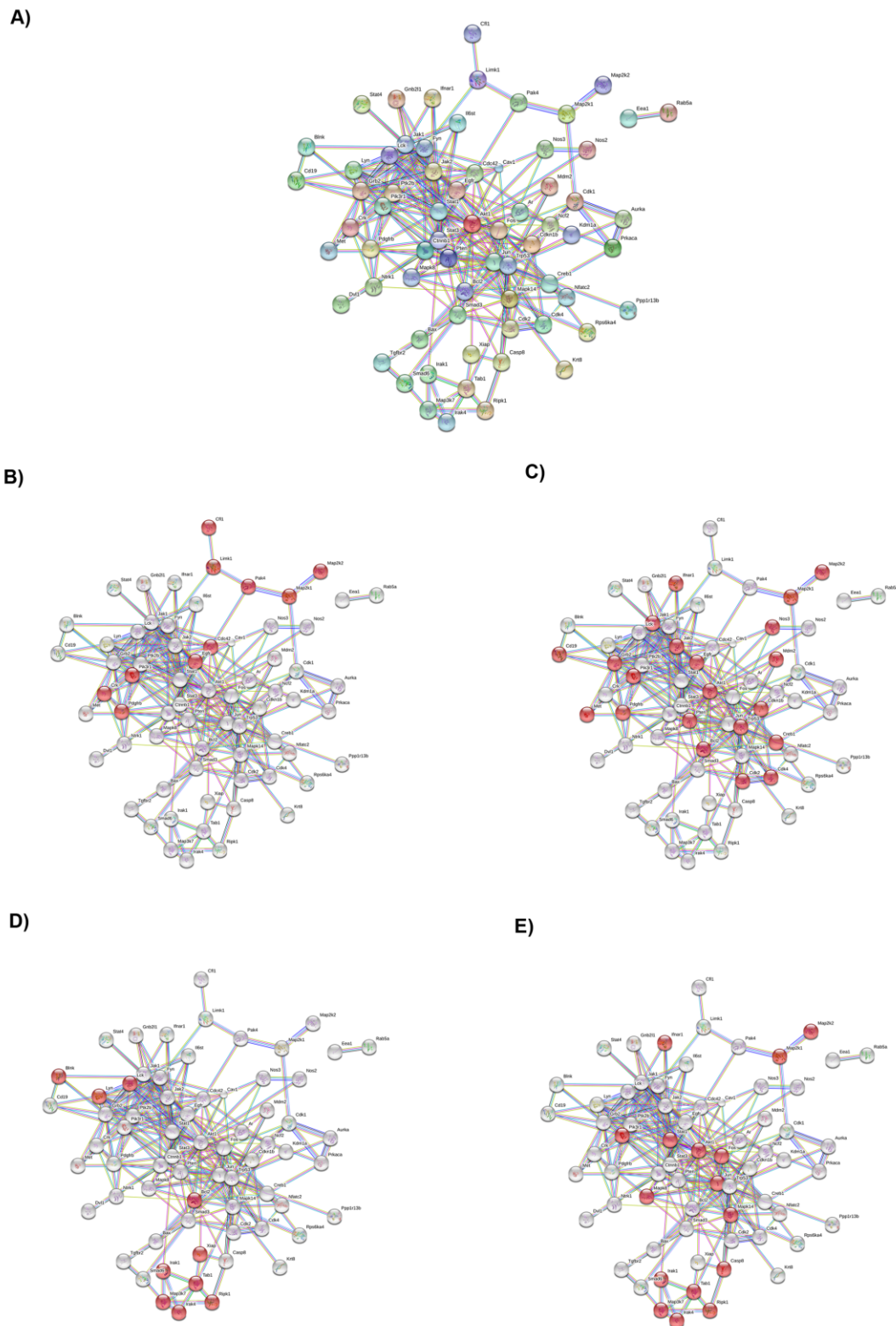
**Figure 1: Animal parameters follow-up with 10ppm of FB1 exposure.**

Figure 2. Gene expression profile of liver and jejunum exposed to FB1. Liver and jejunum tissue from animals exposed for 28 days to FB1, were analyzed with a 60K microarray. Left, heatmap representing differentially expressed probes ( $P < 0.05$ ) between FB1-exposed and control tissue. Red and green indicate values above and below the mean (average Z-score), respectively. Black indicates values close to the mean. Center, protein–protein interaction network built with String-db from the same differentially expressed probes as the heatmap. Right, the top 15 KEGG enriched pathways identified by functional enrichment. (A) Jejunum (B) Liver.



**Figure 2: Gene expression profile of liver and jejunum exposed to FB1.**

Figure 3. Protein-protein interaction (PPI) network built from the differential analysis of the kinome profile in the jejunum of the control group or animals exposed to FB1. (A) Global PPI network involved in the response to FB1 exposure. (B) Protein nodes (highlighted in red) of the global PPI network involved in the actin signaling pathway. (C) Protein nodes (highlighted red) of the global PPI network that are involved in the PI3K-AKT signaling pathway. (D) Protein nodes (highlighted red) of the global PPI network that are involved in the NF-kappa B signaling pathway. (E) Protein nodes (highlighted red) of the global PPI network that are involved in the Toll-like receptor signaling pathway.

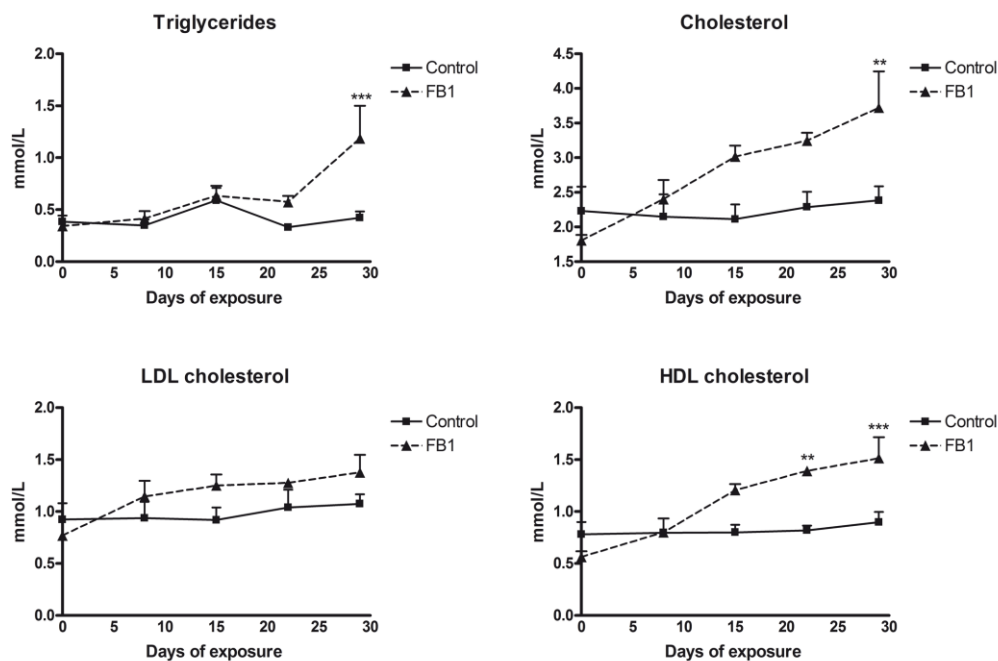


**Figure 3: Protein–protein interaction (PPI) network of the kinome profile in the jejunum**

Figure 4. Protein–protein interaction (PPI) network built from the differential analysis of the kinome profile in the liver of the control group or of animals exposed to FB1. (A) Global PPI network involved in response to FB1 exposure. (B) Protein nodes (highlighted in red) of the global PPI network that are involved in the PI3K-AKT signaling pathway. (C) Protein nodes (highlighted red) of the global PPI network that are involved in the Toll-like receptor signaling pathway. (D) Protein nodes (highlighted red) of the global PPI network that are involved in the NF- $\kappa$ B signaling pathway.

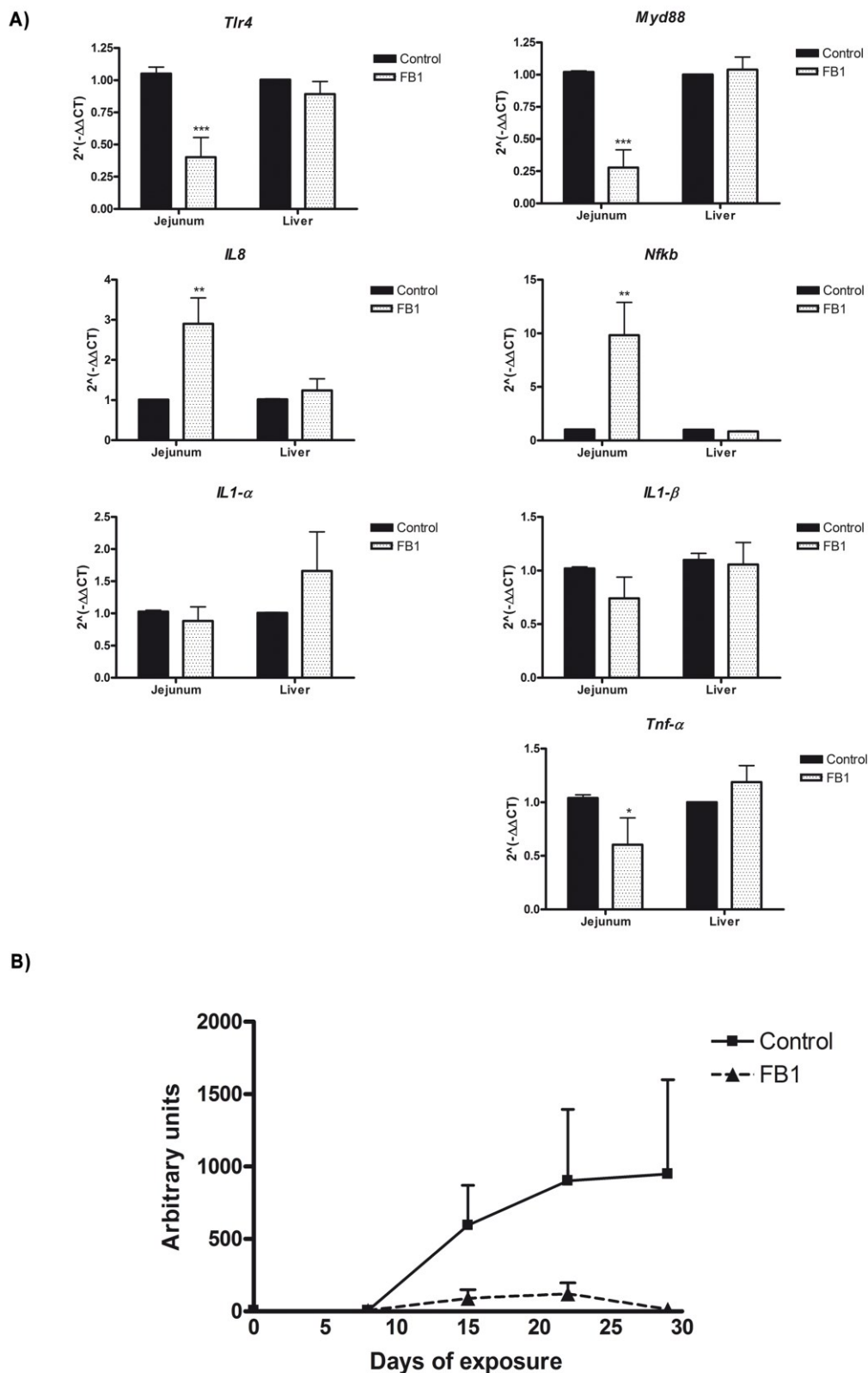


Figure 5. Effect of FB1-exposure on plasma triglycerides and cholesterol (total, LDL, HDL). Data (means  $\pm$  SD of six animals) are plotted with a solid line connecting black solid squares for the control group and a dashed line connecting black solid triangles for the FB1-exposed group. \*, \*\*, and \*\*\* indicate significant differences relative to the control group at  $P < 0.05$ ,  $<0.01$ , and  $<0.001$ , respectively.



**Figure 5: Biochemical analysis of the lipogenic plasma parameters.**

Figure 6. Effect of FB1-exposure on the immune response. (A) Modulation of selected genes involved in immune responses (TLR4: Toll-like receptor 4; MYD88: Myeloid differentiation primary response gene 88; IL-8: Interleukin-8; NF- $\kappa$ B: Nuclear factor kappa B; IL-1a: Interleukin 1-alpha; IL-1b: Interleukin 1-beta; TNF  $\alpha$ : Tumor necrosis factor-alpha). Data (means  $\pm$  SD of six animals) plotted with a black solid bar for control group and white open dotted bar for FB1-exposed group. (B) *Mycoplasma hyopneumoniae* antibody levels. Data (means  $\pm$  SD of six animals) are plotted with a solid line connecting black solid squares for the control group and a dashed line connecting black solid triangles for the FB1-exposed group. \*, \*\*, and \*\*\* indicate significant differences relative to the control group at  $P < 0.05$ ,  $<0.01$ , and  $<0.001$ , respectively.



**Figure 6: Effect of FB1-exposure on the immune response.**

Graphical abstract. FB1 is one of the most spread mycotoxin in the world which induces a broad spectrum of effects in mammals. The molecular mechanism of action of this toxin remaining unclear, so we used a comparative approach with transcriptome and kinome profiles to highlight PP2A and PI3K/AKT as key signaling pathways involved in FB1 toxicity. We assume this key point might be a good target to develop new antimycotoxin strategy in the future.

Table 1. Top-scored differentially expressed genes in FB1-treated porcine jejunum tissue

Gene symbol	Gene name	Fold change	P value
Upregulated genes			
CCND1	Cyclin D1	10.79	0.0098
S100G	S100 calcium binding protein G	6.47	0.0092
FLNA	Filamin A	5.55	0.0004
CKM	Creatine kinase, muscle	4.97	0.0005
ANGPTL4	Angiopoietin-related protein 4	4.89	0.0015
ACTA1	Actin, alpha 1, skeletal muscle	4.88	0.0041
AQP10	Aquaporin 10	4.79	0.0260
HBB	Hemoglobin, beta	4.74	0.0006
SLA-DQB1	SLA-DQ beta1 domain	4.49	0.0002
DES	Desmin	4.45	0.0008
Downregulated genes			
FABP6	Fatty acid binding protein 6, ileal	34.29	0.0005
SPIRE2	Spire homolog 2 ( <i>Drosophila</i> )	10.96	0.0018
BEST2	Bestrophin 2	7.09	0.0005
TAC4	Tachykinin 4 (hemokinin)	4.70	0.0004
MT1A	Metallothionein 1A	4.51	0.0226
OASL	2'-5'-oligoadenylate synthetase-like	4.26	0.0210
SFN	Stratifin	3.96	0.0002
DAD1	Defender against cell death 1	3.30	0.0365
MT1G	Metallothionein 1G	3.16	0.0166
FABP3	Fatty acid binding protein 3, muscle and heart	3.05	0.0026

Table 2. Top-scored differentially expressed genes in FB1-treated porcine liver

Gene symbol	Gene name	Fold change	P
Upregulated genes			
NPG4	Protegrin 4	11.38	0.0013
MEG3	Maternally expressed 3	11.29	0.0005
COL1A2	Collagen, type I, alpha 2	5.74	0.0051
AHSP	Erythroid-associated factor	5.21	0.0380
PR39	Peptide antibiotic PR39	4.74	0.0327
MT1A	Metallothionein 1A	4.55	0.0411
DCN	Decorin	4.29	0.0083
IGF1	Insulin-like growth factor 1	4.19	0.0250
S100A8	S100 calcium binding protein A8	4.04	0.0002
COL3A1	Collagen, type III, alpha 1	4.02	0.0050
Downregulated genes			
S100G	S100 calcium binding protein G	18.93	0.0060
SDS	Serine dehydratase	6.84	0.0156
PDZK1IP1	PDZK1 interacting protein 1	4.33	0.0322
NRG4	Neuregulin 4	4.22	0.0010
IGFBP2	Insulin-like growth factor binding protein 2	4.01	0.0013
mfsd2a	Major facilitator superfamily domain containing 2	3.75	0.0474
ARG1	Arginase, liver	3.03	0.0059
DCPS	Decapping enzyme, scavenger	2.75	0.0391
KCNK5	Potassium channel, subfamily K, member 5	2.70	0.0125
ACSL4	Acyl-CoA synthetase long-chain family member 4	2.65	0.0377

Table 3. Ten top-scored canonical pathways differentially regulated in FB1-treated porcine liver

Ingenuity canonical pathways	Log (P value)	Ratio	Molecules
LXR/RXR Activation	1.24E01	1.87E-01	SCD, APOA4, MSR1, NR1H4, ARG2, PON1, LYZ, CCL2, ITIH4, FASN, SAA1, NGFR, S100A8, LBP, PON3, C3, APOA5, IL1R1, IL33, LY96, IL18, SREBF1, IL1RN, APOC3, ACACA, FGA
Acute Phase Response Signaling	8.35E00	1.38E-01	HAMP, SERPING1, RBP1, HMOX1, MBL2, SOD2, ITIH4, APCS, NGFR, SAA1, LBP, C3, MYD88, C5, IL1R1, CRABP1, IL33, FOS, IL18, MAPK14, RRAS2, C4BPA, IL1RN, CRP, FGA
LPS/IL-1-Mediated Inhibition of RXR Function	7.75E00	1.14E-01	NR1H4, HMGCS2, CHST15, MAOB, ALDH1A3, NGFR, SULT1E1, ACSL4, GSTA1, CPT1C, FABP3, LBP, GSTA2, ACOX2, MYD88, CYP2A7, IL1R1, PAPSS2, SULT2A1, IL33, LY96, IL18, SREBF1, IL1RN, CPT2, ALDH18A1, ABCC3, PPARGC1A
Agranulocyte Adhesion and Diapedesis	6.93E00	1.25E-01	ITGB1, MMP7, SELL, MMP14, ACTA2, CXCL12, C5, IL1R1, IL33, CXCL10, IL18, CLDN5, CCL2, CLDN12, CDH5, CLDN8, IL1RN, CXCR2, CCL21, CLDN14, ACTG2, ACTA1, CCL19, ITGA4
Granulocyte Adhesion and Diapedesis	6.81E00	1.26E-01	ITGB1, MMP7, SELL, MMP14, CXCL12, C5, IL1R1, IL33, CXCL10, IL18, CLDN5, CCL2, CLDN12, CLDN8, CDH5, IL1RN, SDC2, CXCR2, NGFR, CCL21, CLDN14, CCL19, ITGA4
Complement System	6.66E00	2.86E-01	SERPING1, CD59, MBL2, C3, MASP2, C4BPA, C7, C5, C6, CFH
Atherosclerosis Signaling	6.18E00	1.29E-01	APOA4, MSR1, PLA2R1, CXCL12, ALOX12, PDGFC, COL1A2, IL33, PON1, COL1A1, IL18, LYZ, CCL2, IL1RN, APOC3, S100A8, ITGA4, COL3A1
Hepatic Fibrosis/Hepatic Stellate Cell Activation	5.96E00	1.23E-01	ACTA2, IGFBP5, IL1R1, PDGFC, BCL2, COL1A2, COL1A1, LY96, IGF1, CCL2, NGFR, CCL21, TGFA, TGFB3, IGFBP3, LBP, KDR, EGFR, COL3A1
IL-10 Signaling	5.92E00	1.67E-01	TYK2, BLVRB, ARG2, IL1R1, FCGR2B, IL33, HMOX1, FOS, IL18, MAPK14, IL1RN, IL10RB, LBP
STAT3 Pathway	5.55E00	1.62E-01	TGFBR3, TYK2, BMPR2, DDR1, BCL2, MYC, GHR, MAPK14, RRAS2, PIM1, NGFR, KDR, EGFR

Table 4. Ten top-scored canonical pathways differentially regulated in FB1-treated porcine jejunum

Ingenuity Canonical Pathways	Log (P value)	Ratio	Molecules
ILK Signaling	1.03E01	2.19E-01	RELA, FN1, DIRAS3, MYH11, HIF1A, CCND1, EP300, PTEN, ITGB3, VEGFA, AKT1, FLNA, MAPK3, ATF4, PPP2R5C, ACTG2, NOS2, ACTC1, ACTA1, ITGB5, ATM, FBLIM1, CFL1, LIMS2, TNFRSF1A, RHOC, FGFR1, ACTN2, ACTB, FERMT2, CREB3, MAPK9, VIM, CREB3L4, MYL9, PPP2R1A, RHOQ, PTPN11, ACTA2, FLNC, KRT18, PPP2R1B, MMP9
LXR/RXR Activation	8.05E00	2.4E-01	ABCG8, SCD, APOE, RELA, IL1A, APOB, NR1H4, APOA2, CD36, ARG2, PON1, LYZ, CCL2, LCAT, SAA1, FASN, LPL, SERPINA1, LBP, NOS2, CYP51A1, PON3, C3, TNFRSF1A, SERPINF1, IL-18, LDLR, CLU, MMP9
Acute Phase Response Signaling	7.78E00	2.07E-01	HAMP, IL6ST, RELA, SERPING1, IL1A, FN1, APOA2, JAK2, RBP1, NR3C1, HMOX1, IKBKB, IKBKG, AKT1, SOD2, F8, APCS, MAPK3, SAA1, MRAS, SOCS2, SERPINA1, LBP, CHUK, C3, MYD88, TNFRSF1A, C1S, SERPINF1, MAPK9, SOCS4, IL18, PTPN11, C4BPA, C2
Production of Nitric Oxide and Reactive Oxygen Species in Macrophages	6.77E00	1.87E-01	APOE, RELA, APOB, DIRAS3, APOA2, PPP1R3C, ARG2, JAK2, IKBKB, PON1, LYZ, IKBKG, AKT1, MAPK3, SERPINA1, PPP2R5C, CHUK, NOS2, STAT1, ATM, PTPN6, RHOC, TNFRSF1A, FGFR1, MAPK9, IFNGR1, NCF4, RAP1A, IRF1, PPP2R1A, RHOQ, PTPN11, NCF2, CAT, PPP2R1B, CLU
NRF2-mediated Oxidative Stress Response	6.3E00	1.81E-01	ABCC2, DNAJA4, HSPB8, EP300, HMOX1, AKT1, SOD2, SCARB1, ABCC1, MAPK3, VCP, MRAS, ATF4, GSTA1, GCLM, DNAJB1, ACTG2, ACTC1, ACTA1, ATM, GSTA2, MGST1, FGFR1, ACTB, GSTM3, NQO1, MAPK9, TXNRD1, GSTO1, GSR, PTPN11, ACTA2, CAT, DNAJC14, EPHX1
Interferon Signaling	6.12E00	3.61E-01	IFIT3, RELA, MX1, IFNGR1, BAX, JAK2, TAP1, IRF1, BCL2, ISG15, IFIT1, STAT1, IFITM1
Type II Diabetes Mellitus Signaling	5.86E00	2.05E-01	RELA, SLC27A2, CD36, PKM, SMPD1, IKBKB, IKBKG, AKT1, SLC2A2, MAPK3, ABCC8, SOCS2, CHUK, NSMAF, ATM, PPARG, TNFRSF1A, FGFR1, MAPK9, SOCS4, SLC2A4, PTPN11, SLC27A3, ENPP7, ACSL1, PDX1
Leukocyte Extravasation Signaling	5.85E00	1.71E-01	CD99, CLDN11, MMP3, CXCL12, CRK, ITGB3, CLDN4, TIMP1, ACTG2, DLC1, ACTC1, ACTA1, ATM, ITGA4, VAV2, SRC, ACTB, ACTN2, FGFR1, THY1, MMP10, MAPK9, NCF4, RAP1A, BTK, GNAI2, TEC, F11R, CLDN5, PTPN11, CLDN12, ACTA2, NCF2, PECAM1, VAV1, MMP9

Tec Kinase Signaling	5.71E00	1.82E-01	RELA, GTF2I, DIRAS3, TNFSF10, JAK2, GNG11, MRAS, ACTG2, STAT1, ACTC1, ACTA1, ATM, ITGA4, VAV2, TNFRSF21, SRC, GNAS, RHOC, ACTB, FGFR1, MAPK9, GNAZ, BTK, GNAI2, FADD, TEC, RHOQ, PTPN11, ACTA2, MS4A2, VAV1
Aryl Hydrocarbon Receptor Signaling	5.53E00	1.93E-01	RELA, TRIP11, IL1A, CDK4, CCND1, PTGES3, EP300, NR2F1, CTSD, ALDH1L1, CYP1A2, HSP90AB1, CCND3, MAPK3, GSTA1, AHR, ATM, GSTA2, SRC, CYP1A1, MGST1, GSTM3, NQO1, BAX, GSTO1, HSP90AA1, ALDH16A1

Table 5. Modulation of the protein phosphorylation after exposure to FB1 diet

	Jejunum	Number of proteins	Number of phosphorylation sites
More phosphorylated (site of phosphorylation)	14-3-3 $\beta$ (S59); 4E-BP1(S64); auro(T287); Bax(S184); Bcl-2(S87) BLNK (Y178); Cdc2 (T161); CDK4 (S150); CFL1(S2); CREB(S111); Crk (Y221); CTNNB1(S675); DVL1(S679); GP130(S782); EEA1(T431); EGFR(T693); eNOS(S1176); IFNAR1(Y466); IKK-a(S180,S473,T23); iNOS(S745); IRAK1(T387); IRAK4(T208); IRF-7(S471); IIRS-1 (S312); JAK1(Y1034/5); JNK1 (T183); Lyn(Y507); MAPK14(Y322, T179); MDM2(S186/8); Mek1(T385,S217); Mek2(S226; Met(Y100); 53(S15); PDGFRb(Y740); Pyk2(S399); RAB5A(Y205,T202); Rack1(Y194); Ripk1(Y424); sek1(S257,S80); Smad3(S204,S208,T179); Smad6 (S435); TAK1(T178); STAT1(Y701); TAB1(S423,S438); TAK1 (T187); Tgfbr2(S409,Y336)	45	56
Less phosphorylated (site of phosphorylation)	AMPK1(T174); Akt1 (T308); AR (Y363); Casp8 (Y448); CAV1 (Y6,Y14); CAT (Y385); CD19 (Y531); dc2(Y15); Cdc42(Y32); CDK2(T160,Y14,Y179); CFL1(Y139); ERK3(S189); Fos(S362), FYN(Y240); IT2(Y484,Y592); GRb2 (Y209,Y37); IRAK1(T100,T209); Jak2(Y1007,Y119, Y813); Jun (S63); K8(Y267); Lck(Y192); LIMK1(T508); LSD1(S131); MAPK14(T179); MIK3(T277); MSK2(S360,Y132); NFAT1(S326); NFkB-p65(S276); NFkBp105(S337); p27kip1 (Y74); p67phox(S208); PAK4(S474); PI3K p85 $\beta$ (Y605); PIK3R1(Y556); PKACa(S338); PTEN(Y240); Ripk1(Y394); sek1(S2315); STAT1(S708); STAT3(S727,S691); STAT4(Y693); Tgfbr2(Y259); TNIK (T181); TrKA(Y496); XIAP (S87)	45	55
Liver			
More phosphorylated	Akt1(T308); Bax(S184); Bcl-2(S87); Cdc2(T161);	26	28

This article is protected by copyright. All rights reserved.

41

Comment citer ce document :

Régnier, M., Gourbeyre, P., Pinton, P., Napper, S., Laffitte, J., Cossalter, A. M., Bailly, J.-D., Lippi, Y., Bertrand-Michel, J., Bracarense, A. P. F., Guillou, H., Loiseau, N. (Auteur de correspondance), Oswald, I. P. (Auteur de correspondance) (2017). Identification of signaling pathways targeted by the food contaminant FB1: Transcriptome and kinome analysis of samples from

(site of phosphorylation)	CDK2(Y179); EEA1(T431); EGFR(T693); EP300(S2366); Grb10(S150); IRAK4(T208); IRS-1(S616); JAK1(Y1034/5); K8(S74); MK2(Y132); Mnk1(T250); p38-a(T122); p70S6K(T412); PTEN(T382/3/5); Rack1(Y194,Y246); ipk1(Y694,Y384); Shc1(Y349); STAM2(Y371); TAT1(Y701); STMN1(S37); Syk(Y352); TrKA(Y496)		
Less phosphorylated (site of phosphorylation)	A-Raf(T20); AR(Y363); Akt1(S473); CAT (Y385); Cdk4(T172); CHOP(S7); CREB (S111); DVL1(S679); FYN(Y240); HSP27(S78); IKK $\alpha$ (S180); JNK1(T183); JNK2(T183); MAPK14(T149,Y322); MDM2(S186); Mek2(S226); NFAT3(S676); FkB p100(S99); P27kip1(T157); P38d(Y182); p47phox(S359); 67phox(T233); PDK1(S241); PI3Kp85 $\beta$ (Y605); PIK3R1(Y556); PLCG2(Y753); Rab5A(T202); Rack1(Y52); Smad6(S435); STAT3(S727); TAB1(S423); TAK1(T178); TGFBR1(T204)	33	34